Unsteady MHD Slip Flow of a Non-Newtonian Casson Fluid due to Stretching Sheet with Suction or Blowing Effect

A. Mahdy

Department of Mathematics, Faculty of Science, South Valley University, Qena, Egypt

Email: mahdy@svu.edu.eg

ABSTRACT

In this contribution a numerical study is carried out to analyze the effect of slip at the boundary of unsteady two-dimensional MHD flow of a non-Newtonian fluid over a stretching surface having a prescribed surface temperature in the presence of suction or blowing at the surface. Casson fluid model is used to characterize the non-Newtonian fluid behavior. With the help of similarity transformations, the governing partial differential equations corresponding to the momentum and heat transfer are reduced to a set of non-linear ordinary differential equations, which are then solved for local similar solutions using the very robust computer algebra software MATLAB. The flow features and heat transfer characteristics for different values of the governing parameters are graphically presented and discussed in detail. Comparison with available results for certain cases is excellent. The effect of increasing values of the Casson parameter is seen to suppress the velocity field. But the temperature is enhanced with increasing Casson parameter. For increasing slip parameter, velocity increases and thermal boundary layer becomes thinner in the case of suction or blowing.

Keywords: Casson fluid; Slip effect; Unsteady flow; MHD; Suction/Injection.

1. INTRODUCTION

Non-Newtonian fluid flows generated by a stretching sheet have been widely analyzed for the importance in several manufacturing processes such as extrusion of molten polymers through a slit die for the production of plastic sheets, processing of food stuffs, paper production, and wire and fiber coating. On the other hand, convective heat transfer plays a vital role during the handling and processing of non-Newtonian fluid flows.

Mechanics of non-Newtonian fluid flows present a special challenge to engineers, physicists, and mathematicians. Because of the complexity of these fluids, there is not a single constitutive equation which exhibits all properties of such non-Newtonian fluids. In the process, a number of non-Newtonian fluid models have been proposed. The vast majority of non-Newtonian fluid are concerned of the types, e.g., like the power-law and grade two or three (Serdar and Salih Dokuz (2006), Andersson and Dandapat (1992), Sadeghy and Sharifi (2004), Hassanien (1996), Sajid *et al.* (2007, 2009), Keimanesha *et al.* (2011), Rashidi *et al.* (2012)). These simple fluid models have the shortcomings that render results that are not in accordance with

the fluid flows in reality. Power-law fluids are by far the most widely used model to express non-Newtonian behavior in fluids. The model predicts shear thinning and shear thickening behavior. However, it is inadequate in expressing normal stress behavior as observed in die swelling and rod climbing behavior in some non-Newtonian fluids. In order to obtain a thorough cognition of non-Newtonian fluids and their various applications, it is necessary to study their flow behaviors. Due to their application in industry and technology, few problems in fluid mechanics have enjoyed the attention that has been accorded to the flow which involves non-Newtonian fluids. The non-linearity can manifest itself in a variety of ways in many fields, such as food, drilling operations and bio-engineering. The Navier–Stokes theory is inadequate for such fluids, and no single constitutive equation is available in the literature which exhibits the properties of all fluids. Because of the complexity of these fluids, there is not a single constitutive equation which exhibits all properties of such non-Newtonian fluids. Thus, a number of non-Newtonian fluid models have been proposed. The Casson model is a well-known rheological model for describing the non-Newtonian flow behavior of fluids with a yield

stress as Casson (1959). The model was developed for viscous suspensions of cylindrical particles by Reher *et al*. (1969). Regardless of the form or type of suspension, some fluids are particularly well described by this model because of their nonlinear yield-stress-pseudoplastic nature. Examples are blood as Cokelet *et al*. (1963), chocolate by Chevalley (1991), xanthan gum solutions by Garcia-Ochoa and Casas (1994). The Casson model fits the flow data better than the more general Herschel–Bulkley model by Joye (1998) and Kirsanov, and Remizo (1999), which is a power-law formulation with yield stress as Bird *et al*. (1960). For chocolate and blood, the Casson model is the preferred rheological model. It seems increasingly that the Casson model fits the nonlinear behavior of yield-stress-pseudoplastic fluids rather well and it has therefore gained in popularity since its introduction in 1959. It is relatively simple to use, and it is closely related to the Bingham model Bird *et al*. (1960), which is very widely used to describe the flow of slurries, suspensions, sludge, and other rheologically complex fluids as Churchill (1988). Eldabe and Salwa (1995) have studied the Casson fluid for the flow between two rotating cylinders, and Boyd *et al*. (2007) investigated the Casson fluid flow for the steady and oscillatory blood flow. Boundary layer flow of Casson fluid over different geometries is considered by many authors in recent years. Nadeem *et al*. (2012) presented MHD flow of a Casson fluid over an exponentially shrinking sheet. Kumari *et al*. (2011) analyzed peristaltic pumping of a MHD Casson fluid in an inclined channel. Sreenadh *et al*. (2011) studied the flow of a Casson fluid through an inclined tube of non uniform cross-section with multiple stenoses. Mernone and Mazumdar (2002) discussed the peristaltic transport of a Casson fluid. Porwal and Badshah (2012) work on steady blood flow with Casson fluid along an inclined plane influenced by the gravity force. Mukhopadhyay *et. al*. (2013) studied the unsteady two-dimensional flow of a non-Newtonian fluid over a stretching surface having a prescribed surface temperature, the Casson fluid model is used to characterize the non-Newtonian fluid behavior. Abolbashari *et al*. (2015) have been reported an analytical investigation of the fluid flow, heat and mass transfer and entropy generation for the steady laminar non-Newtonian nano-fluid flow induced by a stretching sheet in the presence of velocity slip and convective surface boundary conditions using optimal homotopy analysis method (HAM).

Suction or blowing process has also have their importance in many engineering activities, for example, in the design of thrust bearing and radial diffusers, and thermal oil recovery. Suction is applied to chemical processes to remove reactants. Blowing is used to add reactants, which cool the surface, prevent corrosion or scaling and reduce the drag. In mass transfer cooling, can significantly change the flow field and, as a consequence, affects the heat transfer rate from the plate (see Shridan *et al*. (2006), Chamkha *et al*. (2010), Yih (1998), Tsai *et al*. (2008), Ishak *et al*. (2009)). In addition, a combined free and forced convection flow of an electrically conducting fluid in the presence of a transverse magnetic field is of special technical significance because of its frequent occurrence in many industrial applications such as geothermal reservoirs, cooling of nuclear reactors, thermal insulation, petroleum reservoirs, etc. This type of problem also arises in electronic packages, microelectronic devices during their operations. In recent years, several convection heat transfer and fluid flow problems have received new attention within the more general context of MHD. The purpose of the present investigation is to study the unsteady boundary layer slip flow and heat transfer characteristics of a non-Newtonian Casson fluid along a stretching vertical sheet taking into account the effects suction or injection. Similarity transformation is employed, and the reduced ordinary differential equations are solved numerically. The results of this parametric study are shown graphically and the physical aspects of the problem are highlighted and discussed.

2. FLOW ANALYSIS

Consider laminar MHD boundary layer two-dimensional slip flow and heat transfer of an incompressible, conducting non-Newtonian Casson fluid over an unsteady stretching sheet with suction or blowing effect. A magnetic field of uniform strength B is applied in the $y-$ direction, i.e., normal to the flow direction. The external electric field is assumed to be zero and the magnetic Reynolds number is assumed to be small. Hence, the induced magnetic field is small compared with the externally applied magnetic field. The unsteady fluid and heat flows start at $t=0$. The sheet emerges out of a slit at origin $(x=0, y=0)$ and moves with non-uniform velocity $U(x,t) = ax(1-\gamma t)^{-1}$, where $a>0$; $\gamma \geq 0$ are constants with dimension (time)$^{-1}$, a is the initial stretching rate. The rheological equation of state for an isotropic and incompressible flow of a Casson fluid as (Eldabe and Salwa , 1995; Elbashbeshy and Bazid ,2004)

$$\tau_{ij} = \begin{cases} 2\left(\mu_B + P_y / \sqrt{2\pi}\right)e_{ij}, \ \pi > \pi_c \\ 2\left(\mu_B + P_y / \sqrt{2\pi_c}\right)e_{ij}, \ \pi < \pi_c \end{cases}$$

Here, τ_{ij} is the (i,j)-th component of the stress tensor, $\tau_{ij} = e_{ij}e_{ij}$ and e_{ij} are the (i,j)-th component of the deformation rate, π is the product of the component of deformation rate with itself, π_c is a critical value of this product based on the non-Newtonian model, μ_B is plastic dynamic viscosity of the non-Newtonian fluid, and P_y is the yield stress of the fluid. So, if a shear stress less than the yield stress is applied to the fluid, it behaves like a solid, whereas if a shear stress greater than yield stress is applied, it starts to move. The governing equations of such type of flow are,

in the usual notations

$$\frac{\partial u}{\partial x} + \frac{\partial v}{\partial y} = 0 \quad (1)$$

$$\frac{\partial u}{\partial t} + u\frac{\partial u}{\partial x} + v\frac{\partial u}{\partial y} = \nu\left(1 + \frac{1}{\beta}\right)\frac{\partial^2 u}{\partial y^2} - \frac{\sigma B^2}{\rho}u \quad (2)$$

$$\frac{\partial T}{\partial t} + u\frac{\partial T}{\partial x} + v\frac{\partial T}{\partial y} = \alpha\frac{\partial^2 T}{\partial y^2} + \frac{Q_0}{\rho c_p}\left(T - T_\infty\right) \quad (3)$$

Here, (u,v) are the velocity components in (x,y) directions, respectively, ρ is the density of the fluid, σ is the electrical conductivity, ν is the kinematic viscosity, and α is the thermal diffusivity of the fluid, c_p is the specific heat at constant pressure, Q_0 is the heat generation or absorption coefficient. T is the temperature of the fluid inside the thermal boundary layer. The relevant boundary conditions of the governing equations are

$$y = 0: \quad u = U(x,t) + L\left(\frac{\partial u}{\partial y}\right)$$

$$v = V, \quad T = T_w(x,t)$$

$$y \to \infty: \quad u \to 0, \quad T \to T_\infty \quad (4)$$

where $\quad T_w = T_\infty + \dfrac{ax^2 T_0(1-\gamma t)^{-3/2}}{2\nu} \quad$ is the temperature at the sheet and T_0 is a (positive or negative) reference temperature (slit temperature at $x = 0$). T_∞ is the constant free stream temperature, L is the slip length, The expressions for $U(x,t)$ and $T_w(x,t)$ are valid for time $t < \gamma^{-1}$. Now, in order to obtain a similarity solution of the problem we introduce the following non-dimensional similarity variables:

$$\eta = \sqrt{\frac{a}{\nu(1-\gamma t)}}\, y, \quad \psi = \sqrt{\frac{\nu a}{1-\gamma t}}\, xf(\eta),$$

$$\quad (5)$$

$$T = T_\infty + \left[\frac{ax^2 T_0(1-\gamma t)^{-3/2}}{2\nu}\right]\theta(\eta)$$

where the stream function ψ satisfies the continuity equation and defines in the usually way as $u = \partial\psi / \partial y$, $v = -\partial\psi / \partial x$, η is the dimensionless similarity variable. With the change of variables (5), Eq. (1) is identically satisfied and Eqs. (2)–(4) are transformed to

$$\left(1 + \beta^{-1}\right)f''' + ff'' - f'^2 - Mnf'$$

$$-A\left(f' + 2^{-1}\eta f''\right) = 0 \quad (6)$$

$$\Pr^{-1}\theta'' + f\theta' - 2f'\theta + \lambda\theta$$

$$-2^{-1}A\left(\eta\theta' + 3\theta\right) = 0 \quad (7)$$

The transformed boundary conditions are turn into

$$\eta = 0: \quad f' = 1 + \delta f'', \quad f = S, \quad \theta = 1$$

$$\eta \to \infty: \quad f' \to 0, \quad \theta \to 0 \quad (8)$$

Here prime denotes ordinary differentiation with respect to the similarity variable η.

In addition, $S = -V\left((1-\gamma t)/(\nu a)\right)^{-1/2}$, $S > 0$ (i.e. $V < 0$) corresponding to mass suction and $S < 0$ (i.e. $V > 0$) corresponding to mass injection, $\delta = L(a/\nu(1-\gamma t))^{-1/2}$ is the dimensionless parameter. Moreover, $\Pr = \nu/\alpha$, $Mn = \sigma B^2(1-\gamma t)/(\rho a)$, $A = \gamma/a$ and $\lambda = Q_0(1-\gamma t)/(a\rho c_p)$ are the Prandtl number, magnetic field parameter, dimensionless parameter unsteadiness parameter and heat generation or absorption parameter. In addition, the exact solution of Eq. (6) subject to the corresponding boundary conditions for steady case i.e. for $A = 0$ and non slip flow with $Mn = S = 0$ is given

$$f(\eta) = \sqrt{1 + \beta^{-1}}\left(1 - e^{-\frac{\eta}{\sqrt{1+\beta^{-1}}}}\right)$$

Expressions for the local Nusselt number Nu is

$$Nu = \frac{xq_w}{k(T_w - T_\infty)}, \quad q_w = -k\left.\frac{\partial T}{\partial y}\right|_{y=0}$$

Thus $Nu\,\mathrm{Re}^{-1/2} = -\theta'(0)$

where $\mathrm{Re} = \dfrac{Ux}{\nu}$ is the local Reynolds number.

3. RESULTS AND DISCUSSION

The obtained similarity system (6) - (8) is non-linear, coupled, ordinary differential equations, which possess no closed-form solution. Therefore, the system of equations (6)–(7), along with the boundary conditions (8) are solved numerically by means the very robust symbolic computer algebra software matlab employing the routine bvpc45. The relative tolerance was set to10-6. In this method, we have chosen a suitable finite value of $\eta \to \infty$ namely $\eta_\infty = 25$. The guess should satisfy the boundary conditions of the problem and reveal the behavior of the solution. However, it is difficult to come up with a sufficiently good guess for the solution of the system of the ordinary differential equations (6) and (7) in the case of opposing flow. To overcome this difficulty, we start with a set of parameter values for which the problem is easy to be solved. Then, we use the obtained result as initial guess for the solution of the problem with small variation of the parameters. This is repeated until

the right values of the parameters are reached.

In addition, to validate the method used in this study and to judge the accuracy of the present analysis, comparison with available results of Chamkha *et al*. (2010) and Sharidan *et al*. (2006) corresponding to the skin-friction coefficient f_w'' for unsteady flow of viscous incompressible fluid is made (Table 1) and found in excellent agreement. In order to get a clear insight of the behavior of velocity and temperature fields for non-Newtonian Casson fluid, a comprehensive numerical computation is carried out for various values of the parameters that describe the flow characteristics, and the results are reported graphically. Figures 1 and 2 illustrate the behavior of x -component of the translational velocity and temperature distributions, respectively, for different values of slip parameter. The slip parameter δ measures the amount of slip at the surface. It is observed that, the velocity distribution decreases with the increasing values of slip parameter. Consequently, with the increase of slip parameter the thickness of boundary layer increases. It can further be noted that as $\delta \to \infty$, the velocity of the fluid at the surface will coincide with the free stream velocity of the fluid, because if we increase the slip parameter δ to a value tending to infinity then the boundary layer structure will disappear. Moreover, the temperature distribution increases with increasing the slip parameter.

Table 1 The values of f_w'' for various values of unsteadiness parameter A for Newtonian fluid

A	Chamkha *et al*. (2010)	Sharidan *et al*. (2006)	Present stuy
0.8	-1.261512	-1.261042	-1.261012
1.2	-1.378052	-1.377722	-1.377842
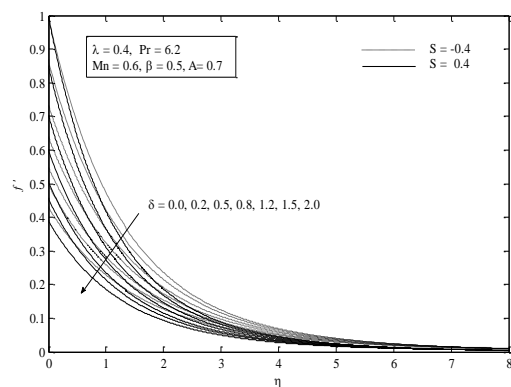
Fig. 1. Velocity profile for various δ .
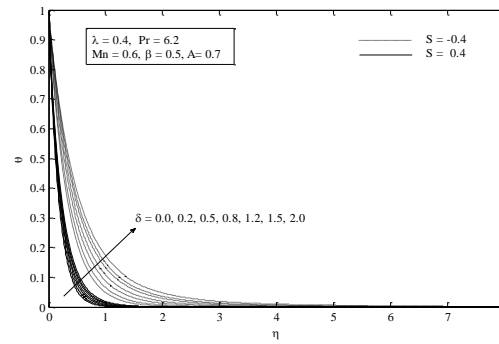

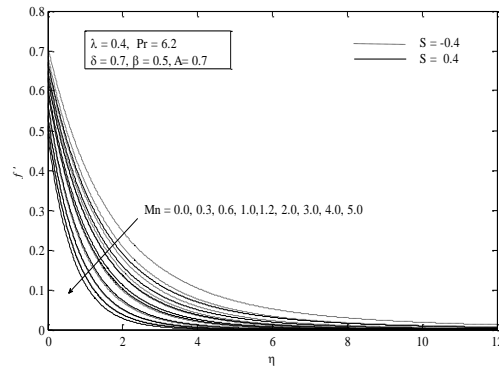**Fig. 2. Temperature profile for various δ .**

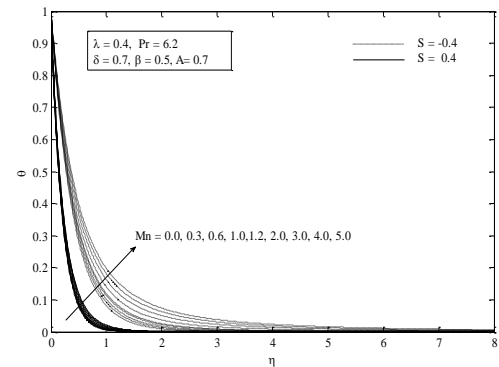**Fig. 3. Velocity distribution for various Mn .**

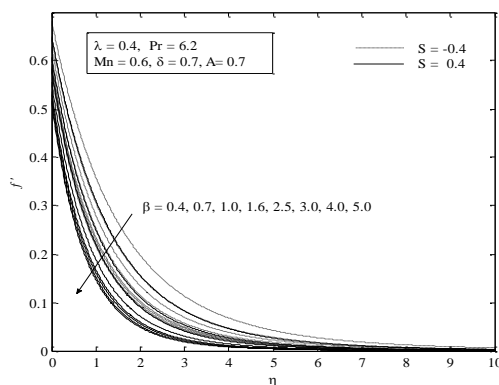**Fig. 4. Temperature distribution for various Mn .**

Fig. 5. Velocity distribution for various β .

Figures 3 and 4, respectively, depict the effects of the magnetic field parameter Mn on the fluid velocity and temperature distributions, considering the cases of wall mass suction and wall mass injection. Application of a magnetic field normal to an electrically-conducting fluid has the tendency to produce a drag-like force called the Lorentz force which acts in the direction opposite to that of the flow, causing a flow retardation effect. This causes the fluid velocity to decrease. However, this decrease in flow speed is accompanied by corresponding increases in the fluid thermal state level.

These behaviors are clearly depicted in the decrease in the fluid velocity and the increase in the fluid temperature in figures 3-4. Furthermore, the magnetic parameter tends to decrease velocity gradient at the wall and increase temperature gradient as seen in Figs. 17 and 18. The velocity gradient as well as temperature gradient tends to decreases or increases rapidly at first, then gradually levels off as the non-Newtonian Casson parameter is increased. It is clear from these figures that both of f_w'' and $-\theta_w'$ decrease with increasing values of the magnetic field parameter. Influences of Casson parameter β on velocity and temperature distributions for unsteady motion are clearly depicted in Figs. 5 and 6, respectively considering wall mass suction and wall mass injection effects (i.e. $S = 0.4, -0.4$). The same type of behavior of velocity with increasing β is noted. The effect of increasing values of β is to reduce the velocity, and hence, the boundary layer thickness decreases. The increasing values of the Casson parameter i.e. the decreasing yield stress (the fluid behaves as Newtonian fluid as Casson parameter becomes large) suppress the velocity field. It is observed that $f'(\eta)$ and the associated boundary layer thickness are decreasing function of β . The velocity curves in Fig. 5 show that the rate of transport is considerably reduced with the increase of β . The effect of increasing β leads to enhance the temperature field for unsteady motion (Fig. 6). This effect is more pronounced for steady motion. The thickening of the thermal boundary layer occurs due to increase in the elasticity stress parameter. It can also be seen from Fig. 5 that the momentum boundary layer thickness decreases as β increases and hence induces an increase in the absolute value of the velocity gradient at the surface.

Figures 7 and 8 exhibit the velocity and temperature distributions, respectively for several values of unsteadiness parameter A . It is observed that the velocity along the sheet decreases initially with the increase in unsteadiness parameter A , and this implies an accompanying reduction of the thickness of the momentum boundary layer near the wall. The steady case is obtained when $A = 0$.
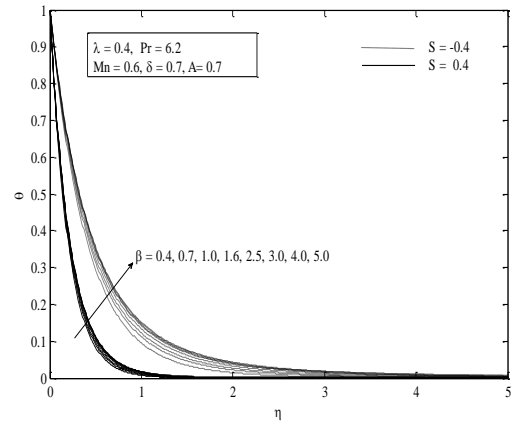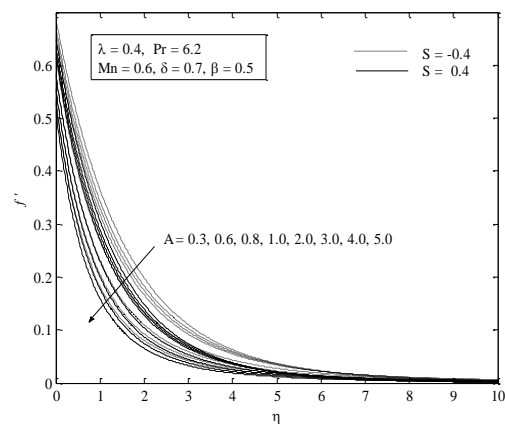

Fig. 6. Temperature distribution for various β **.**

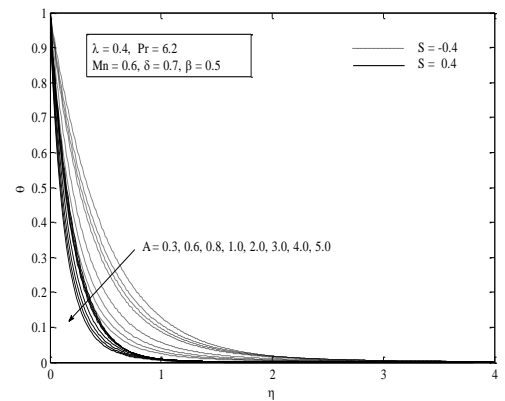**Fig. 7. Velocity distribution for various** A **.**

Fig. 8. Temperature distribution for various A **.**

Furthermore, it is noticed that the temperature at a particular point is found to decrease significantly with increasing unsteadiness parameter. The effect of effect of heat generation or absorption parameter λ on the temperature distributions is shown in Fig. 9. It is clear that as the heat generation or absorption parameter increases the temperature of the fluid increases as well as the temperature gradient increases (Fig. 20).
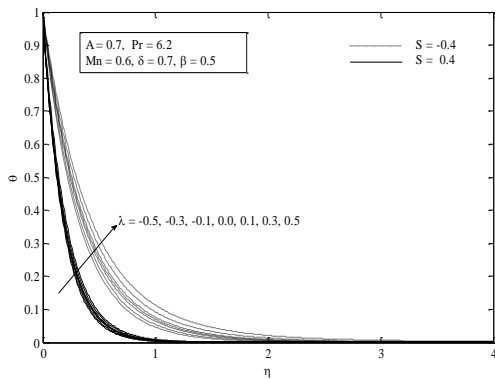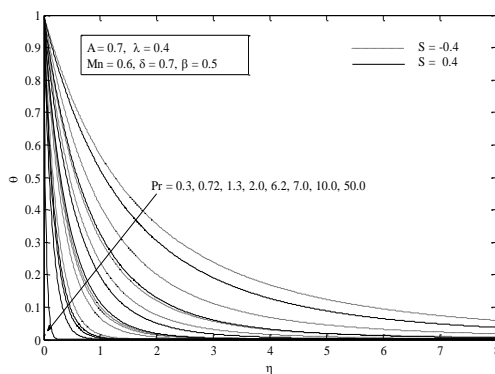
Fig. 9. Temperature distribution for various λ **.**

Fig. 10. Temperature distribution for various
Pr .

Fig. 11. Velocity distribution for various S **.**
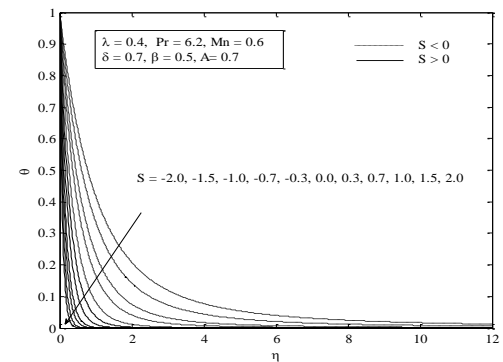
Fig. 12. Temperature distribution for various S **.**
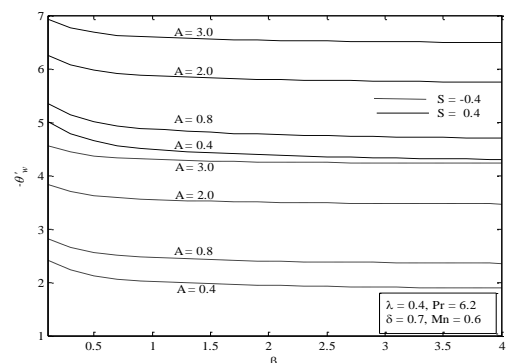
Fig. 13. Variation of temperature gradient with
A **.**

Figure 10 shows the behavior of the temperature distributions for the variation of Prandtl number, Prandtl number signifies the ratio of momentum diffusivity to thermal diffusivity. It is seen that the temperature decreases with increasing Pr . Moreover, the thermal boundary layer thickness decreases by increasing Prandtl numbers. Wall temperature gradient is negative for all values of Prandtl number as seen from Fig. 19 which means that the heat is always transferred from the surface to the ambient fluid. An increase in Prandtl number reduces the thermal boundary layer thickness. Fluids with lower Prandtl number will possess higher thermal conductivities (and thicker thermal boundary layer structures), so that heat can diffuse from the sheet faster than for higher Pr fluids (thinner boundary layers). Figures 11 and 12 display the effects of suction/blowing parameter S on velocity and temperature fields. With increasing S , fluid velocity is found to decrease. That is, the effect of S is to decrease the fluid velocity in the boundary-layer and in turn, the wall shear stress decreases. The increase in S causes thinning of the boundary layer. However, temperature at a point is found to decrease with increasing S . This causes a decrease in the rate of heat transfer.
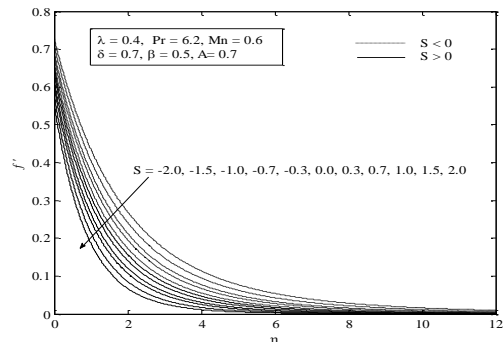
The behavior of rate of heat transfer (from the sheet to the fluid) decreases with increasing A as observed from Fig. 13. As the unsteadiness parameter A increases, less heat is transferred from the sheet to the fluid; hence, the temperature $\theta(\eta)$ decreases (Fig. 8). Since the fluid flow is caused solely by the stretching sheet, and the sheet surface temperature is higher than free stream temperature, the velocity and temperature distributions decrease with increasing η . It is important to note that the rate of cooling is much faster for higher values of unsteadiness parameter, whereas it may take longer time for cooling during steady flows. Moreover, Fig. 14 displays the influences of unsteadiness parameter A and Casson parameter β on velocity gradient at the wall f_w'' . Magnitude of f_w'' related to skin-friction coefficient decreases with increasing unsteadiness

parameter A and also with Casson parameter β, but the magnitude of temperature gradient at the surface decreases for β and A. A drop in skin-friction as investigated in this paper has an important implication that in free coating operations and elastic properties of the coating formulations may be beneficial for the whole process. This means that less force may be needed to pull a moving sheet at a given withdrawal velocity, or equivalently higher withdrawal speeds can be achieved for a given driving force resulting in, increase in the rate of production. Figures 15 and 16 illustrate the effect of slip parameter on velocity and temperature gradient, respectively. As it is illustrated, both of velocity and temperature gradient increase with the increase of slip flow parameter.
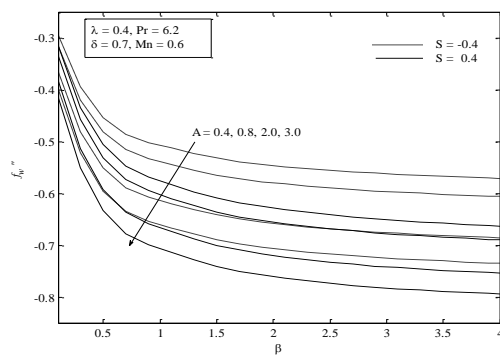

Fig. 14. Variation of velocity gradient for various A.
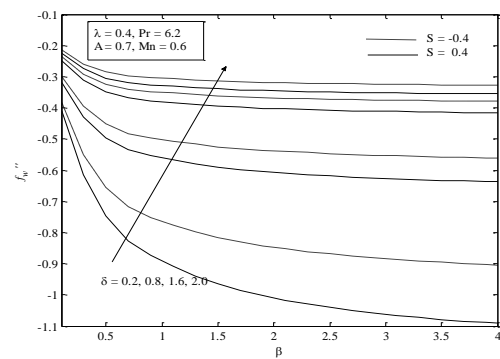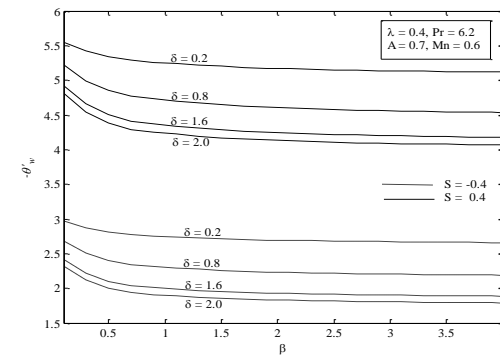

Fig. 15. Variation of velocity gradient for various δ.

Fig. 16. Variation of temperature gradient with δ.

4. CONCLUSIONS

In this paper, the mechanical and thermal properties of unsteady MHD boundary layer slip flow of a non-Newtonian Casson fluid past a vertical stretching surface taking into account the wall mass suction or injection and heat generation or absorption effects have been investigated systemically. With the help of appropriate similarity transformation, the governing time dependent boundary layer equations for momentum and thermal energy are reduced to coupled non-linear ordinary differential equations which are then solved numerically. Results for the velocity and temperature distributions as well as velocity gradient f_w'', temperature gradient $-\theta_w'$ are presented for representative governing parameters. As a summary, we can conclude that

■ Fluid velocity decreases initially due to increase in unsteadiness parameter; temperature also decreases significantly in this case.

■ The effect of increasing values of the Casson parameter is to suppress the velocity field, whereas the temperature is enhanced with increasing Casson parameter. Moreover, Slip parameter and magnetic field parameter have the same effects.

■ Both of f_w'' and $-\theta_w'$ increase with the increase of slip flow parameter, whereas the magnetic field and unsteadiness parameters have an opposite effect. In addition, f_w'' decreases while $-\theta_w'$ increases with increasing Casson parameter.

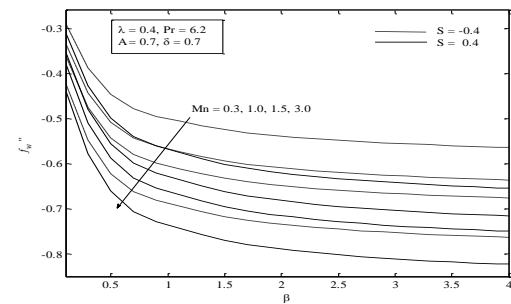■ Prandtl number can be used to increase the rate of cooling in conducting flows.

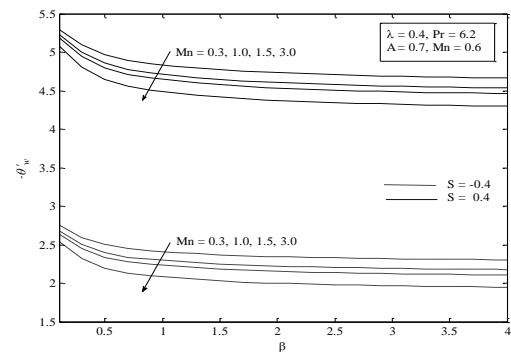**Fig. 17. Variation of velocity gradient with Mn.**
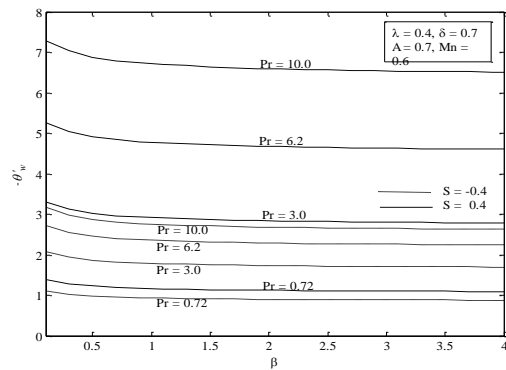

Fig. 18. Variation of temperature gradient with Mn.
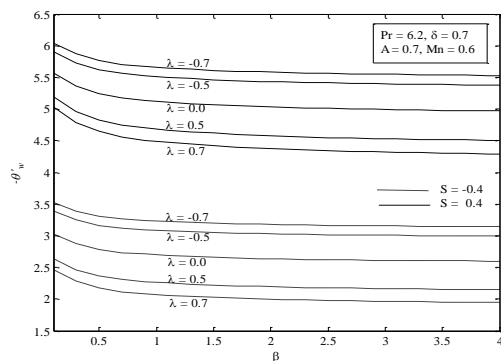
Fig. 19. Variation of temperature gradient with Pr .

Fig. 20. Variation of temperature gradient with λ .

REFERENCES

Abolbashari, M. H., N. Freidoonimehr, F. Nazari and M. M. Rashidi (2015). Analytical modeling of entropy generation for Casson nano-fluid flow induced by a stretching surface. *Advanced Powder Technology*

Andersson, H. I. and B. S. Dandapat. (1992). Flow of a power law fluid over a stretching sheet, Appl. *Anal Continuous Media* 1, 339–347.

Bird, R. B., W. E. Stewart and E. N. Lightfoot (1960). *Transport Phenomena*, Wiley, New York 94–95, 104–105.

Boyd, J., J. M. Buick and S. Green. (2007). Analysis of the Casson and CarreauYasuda non-Newtonian blood models in steady and oscillatory flow using the lattice Boltzmann method. *Phys. Fluids* 19, 93–103.

Casson, N. and C. C. Mills (1959). *Rheology of Disperse Systems*, Pergamon, New York, Ch. 5.

Chamkha, A. J., A. M. Aly and M. A. Mansour (2010). Similarity solution for unsteady heat and mass transfer from a stretching surface embedded in a porous medium with suction/injection and chemical reaction effects. *Chem. Eng. Commun*. 197, 846–858.

Chevalley, J. (1991). An adaptation of the Casson equation for the rheology of chocolate, *J. Texture Stud*. 22, 219–229.

Churchill, S. W. (1988). *Viscous Flows: The Practical Use of Theory*, Butterworths, Boston, Ch. 5.

Cokelet, G. R. (1963). The rheology of human blood—measurement near and at zero shear rate Trans. *Soc. Rheol* 7, 303–317.

Elbashbeshy, E. M. A. and M. A. A. Bazid (2004). Heat transfer over an unsteady stretching surface. *Heat Mass Transfer* 41, 1-4.

Eldabe, N. T. M. and M. G. E. Salwa (1995). Heat transfer of MHD non-Newtonian Casson fluid flow between two rotating cylinder, *J. Phys. Soc. Jpn*. 64, 41–64.

Garcia-Ochoa, F. and J. A. Casas. (1994). Apparent yield stress in xanthan gum solutions at low concentrations. *Chem. Eng. J*. 53, B41–B46.

Hassanien, I. A. (1996). Flow and heat transfer on a continuous flat surface moving in a parallel free stream of power-law fluid. *Appl. Model* 20, 779–784.

Ishak, A., R. Nazar and I. Pop. (2009). Heat transfer over an unsteady stretching permeable surface with prescribed wall temperature Nonlinear Anal. *Real World Appl*. 10, 2909–2913.

Joye, D. D. (1998). in: Hazardous and Industrial Wastes, *Proc. 30th Mid-Atlantic Industrial Waste Conf*., Technomic Publ. Corp., Lancaster, PA/Basel 567–575.

Keimanesha, M., M. M. Rashidi, A. J. Chamkha and R. Jafari (2011). Study of a Third grade non-Newtonian fluid flow between two parallel plates using the multi-step differential transform method. *Computers and Mathematics with Applications* 62, 2871–2891.

Kirsanov, E. A. and S. V. Remizov. (1999). Application of the Casson model to thixotropic waxy crude oil. *Rheol. Acta* 38, 172–176.

Kumari, S. V. H. N. K., M. V. R. Murthy, M. C. K. Reddy and Y. V. K. R. Kumar. (2011). Peristaltic pumping of a magnetohydrodynamic Casson fluid in an inclined channel. *Adv. Appl. Sci. Res*. 2 (2), 428–436.

Mernone, A. V. and J. N. Mazumdar (2002). A mathematical study of peristaltic transport of a Casson fluid. *Math. Comp. Mod*. 35, 895–912.

Nadeem, S., R. U. Haq and C. Lee. (2012). MHD flow of a Casson fluid over an exponentially shrinking sheet. *Scientia Iranica* 19, 1550–1553.

Porwal, P. and V. H. Badshah. (2012). Analysis of steady blood flow with Casson fluid along an inclined plane influenced by the gravity force. *Int. J. Theor. Appl*. Sci. 4(2), 76–81.

Rashidi, M. M., M. T. RasteGari, M. Asadi and O. Anwar Beg (2012). A Study of non-Newtonian flow and heat transfer over a non-isothermal wedge using the homotopy analysis method. *Chem. Eng. Comm*. 199, 251-256.

Reher, E. O., D. Haroske and K. Kohler. (1969). *Chem. Technol*. 21(3), 137– 143.

Sadeghy, K. and M. Sharifi (2004). Local similarity solution for the flow of a 'second-grade' viscoelastic fluid above a moving plate. *Int. J. Nonlinear Mech.* 39, 1265–1273.

Sajid, M., I. Ahmad, T. Hayat and M. Ayub (2009). Unsteady flow and heat transfer of a second grade fluid over a stretching sheet. *Commun. Nonlinear Sci. Num. Simul*. 14, 96–108.

Sajid, M., T. Hayat and S. Asgharm. (2007). Non-similar analytic solution for MHD flow and heat transfer in a third-order fluid over a stretching sheet. *Int. J. Heat Mass Transfer 50*, 1723–1736.

Serdar, B. and M. Salih Dokuz. (2006). Three-dimensional stagnation point flow of a second grade fluid towards a moving plate. *Int. J. Eng. Sci*. 44, 49–58.

Sharidan, S., T. Mahmood and I. Pop. (2006). Similarity solutions for the unsteady boundary layer flow and heat transfer due to a stretching sheet. *Int. J. Appl. Mech. Eng*. 11, 647–54.

Sreenadh, S., A. R. Pallavi and B. h. Satyanarayana. (2011). Flow of a Casson fluid through an inclined tube of non-uniform cross section with multiple stenoses. *Adv. Appl. Sci. Res*. 2(5), 340–349.

Swati Mukhopadhyay, De Prativa Ranjan, Krishnendu Bhattacharyya and G. C. Layek. (2013). Casson fluid flow over an unsteady stretching surface. *Ain Shams Eng. J.* 4, 933-938.

Tsai, R., K. H. Huang and J. S. Huang (2008). Flow and heat transfer over unsteady stretching surface with a non-uniform heat source. Commun. *Heat Mass Transfer* 35, 1340–1343.

Yih, K. A. (1998). Uniform suction/blowing effect on forced convection about a wedge: uniform heat flux. *Acta Mech*. 128, 173–181.